

STUDY OF THE FUSION-FISSION PROCESS IN THE $^{35}\text{Cl}+^{24}\text{Mg}$ REACTION

C. Beck, R. Nouicer, D. Mahboub, B. Djerroud^a R.M. Freeman, A. Hachem^b

T. Matsuse^c

*Institut de Recherches Subatomiques, Institut National de Physique Nucléaire et de Physique des
Particules - Centre National de la Recherche Scientifique/Université Louis Pasteur, B.P.28,
F-67037 Strasbourg Cedex 2, France*

Sl. Cavallaro, E. De Filippo, G. Lanzaó, A. Pagano and M.L. Sperduto

*Dipartimento di Fisica dell'Università di Catania, INFN and LNS Catania, I-95129 Catania,
Italy*

R. Dayras, E. Berthoumieux, R. Legrain, E. Pollacco

DAPNIA/SPhN, C.E. Saclay, F-91191 Gif sur Yvette Cedex, France

(August 22, 2019)

Abstract

Fusion-fission and fully energy-damped binary processes of the $^{35}\text{Cl}+^{24}\text{Mg}$ reaction were investigated using particle-particle coincidence techniques at a ^{35}Cl bombarding energy of $E_{lab} \approx 8$ MeV/nucleon. Inclusive data were also taken in order to determine the partial wave distribution of the fusion process. The fragment-fragment correlation data show that the majority of events arises from a binary-decay process with a relatively large multiplicity of secondary light-charged particles emitted by the two primary excited fragments in the exit channel. No evidence is observed for ternary-breakup processes, as expected from the systematics recently established for incident energies below 15 MeV/nucleon and for a large number of reactions. The binary-process results are compared with predictions of statistical-model calculations. The calculations were performed using the Extended Hauser-Feshbach method, based on the available phase space at the scission point of the compound nucleus. This new method uses temperature-dependent level densities and its predictions are in good agreement with the presented experimental data, thus consistent with the fusion-fission origin of the binary fully-damped yields.

PACS numbers: 25.70.Jj, 24.60.Dr, 25.70.Gh, 25.70.-z

I. INTRODUCTION

The heavy-ion reactions are rather well classified at low bombarding energies ($E_{lab} \leq 10$ MeV/nucleon). The fusion-evaporation (FE) process yield constitutes the major part of the total reaction cross section with one heavy fragment namely the compound nucleus (CN). Binary reaction classes such as fusion-fission, deep-inelastic and quasi-elastic scatterings resulting in exit channels with two heavy fragments are also of importance. On the other hand reactions which produce three or more heavy fragments are known to be strongly suppressed in this energy regime. During the last two decades, considerable effort has been devoted to the understanding of the binary-reaction processes in heavy-ion collisions within the framework of a systematic study of the fusion-fission process (FF) for **light-mass** ($20 \leq A_{CN} \leq 60$) composite systems [1–13]. It has been shown for example that entrance-channel effects do not play a significant role in the binary-decay processes of the ^{47}V nucleus as populated by three studied entrance channels ($^{35}\text{Cl}+^{12}\text{C}$ [3,6], $^{31}\text{P}+^{16}\text{O}$ [5] and $^{23}\text{Na}+^{24}\text{Mg}$ [7]) at comparable excitation energies and angular momenta. Similar conclusions can be reached for the neighbouring ^{48}Cr di-nuclear system as formed also by three different entrance channels [8,11] and even for lighter systems such as ^{27}Al [9] or ^{31}P [13]. This demonstrates that in each case the CN is formed after a complete equilibration of the mass-asymmetry and the shape degrees of freedom. Further, transition-state model [1,4] calculations describe well the properties of the binary-decay channels and thus suggest a FF origin. The occurrence of FF rather than orbiting in certain light-mass systems has been the subject of large number of discussions [1,4–7,13,14]. These have led, in most cases, to the conclusion [1] that FF has to be taken into account when exploring the limitations of the complete fusion (CF) process at large angular momenta and high excitation energies.

In the recent past a complete and systematic investigation of the $^{35}\text{Cl}+^{24}\text{Mg}$ reaction [15–18] leading to the ^{59}Cu compound nucleus was carried out. In this paper we first briefly report on new results of inclusive measurements on binary-reaction yields of $^{35}\text{Cl}+^{24}\text{Mg}$ at a

bombarding energy $E_{lab}(^{35}\text{Cl}) = 275$ MeV. The main focus will be on the fragment-fragment correlation data that have been collected to check the relative importance of binary breakup processes as compared to mechanisms other than secondary particle emission at the high excitation energy ($E_{CN}^* \approx 125$ MeV) in the compound system reached in this reaction. Parts of the preliminary analysis of this experiment have been reported recently in a Short Note [18].

The evidence of ternary breakup processes [19–22] has been primarily found at higher bombarding energies ($E_{lab} \geq 10$ MeV/nucleon) leading to their interpretation as an intermediate mechanism, sandwiched between the binary reactions that dominate at energies close to the interaction barrier and the fragmentation process that occurs when the energy brought into the compound system becomes comparable to the total nuclear binding energy. The unambiguous observation of ternary breakup processes is restricted to certain heavier systems [19,22] where, following a first-step binary decay, one of the reaction products has a sufficiently low fission barrier to allow its subsequent breakup. At bombarding energies close to or above 20 MeV/nucleon this concept of sequential fission becomes inadequate as the time delay between successive breakup steps becomes indistinguishable from the prompt fragmentation. For lighter systems and at lower energies the evidence of sequential fission is limited and, to some extent, contradictory. Boccaccio et al. [23] have claimed to see evidence for a strong ternary breakup yield in several reactions at 5.6 MeV/nucleon and suggest that their data are consistent with a two-step mechanism. With similar experimental sensitivity, however, we find no evidence for a ternary decay mechanism in a somewhat lighter mass system using the $^{35}\text{Cl}+^{12}\text{C}$ reaction at ≈ 8 MeV/nucleon [24]. A more recent experiment was performed in order to explore the ternary breakup of the ^{48}Cr nucleus into three ^{16}O fragments [25]. This study was motivated by the renewed interest in the role of clustering in light nuclei and a linear chain configuration of three- ^{16}O cluster-like is predicted in ^{48}Cr by both the cluster model [26] and macroscopic energy calculations [27]. No supportive evidence was found via the $^{24}\text{Mg}+^{24}\text{Mg}$ entrance channel [25] but other studies are underway by using alternative reactions such as $^{36}\text{Ar}+^{12}\text{C}$ [28]. As a matter of fact sequential

light-fragment emissions from the reaction fragments can lead to large undetected nuclear charge deficits between the observed and entrance-channel total charges rather than a third big fragment.

The nuclear charge deficits in the present measurement of the $^{35}\text{Cl}+^{24}\text{Mg}$ reaction are extracted from the coincidence data in order to verify that they follow the systematic trend that we have established with previously published results [24], thus confirming the binary nature of the reaction. No evidence is seen for the onset of ternary processes for incident energies lower than 10 MeV/nucleon.

The secondary and sequential light-charged particle (LCP) and/or neutron emission from the fully accelerated binary-decay fragments increases with incident energy as the excitation energy imparted to the primary fragments increases. Nevertheless, the properties of the primary fission fragments can be deduced, even at energies as high as 275 MeV, by using the coincident data. As found for the $^{35}\text{Cl}+^{12}\text{C}$ reaction at the same incident energy [24] and at lower energies studied [3,6] the hypothesis of CN formation followed by a statistical decay is supported by the present $^{35}\text{Cl}+^{24}\text{Mg}$ data.

The experimental techniques are briefly described in the next Section. The experimental results of the single and coincidence measurements of the $^{35}\text{Cl}+^{24}\text{Mg}$ reaction are presented in Sect.III. The results are then discussed in Sect.IV within the framework of a FF picture based upon the scission point approximation which determines the fission decay rates. This statistical model is actually an extension of the Hauser-Feshbach formalism which uses temperature-dependent level densities. Transition-state model calculations are also presented for the sake of comparison

II. EXPERIMENTAL PROCEDURES

The investigation of the $^{35}\text{Cl}+^{24}\text{Mg}$ reaction was achieved at the Saclay Booster Tandem facility by means of standard kinematical coincidence techniques [6]. Preliminary results of this coincident experiment have been published in a recent Short Note [18]. Further details of the experimental methods can be found elsewhere [24] in the experimental descriptions of a similar measurement performed for the study of the $^{35}\text{Cl}+^{12}\text{C}$ reaction.

The experiment was carried out with a 275 MeV pulsed beam, provided by the Saclay post-accelerator, focused onto a $255\ \mu\text{g}/\text{cm}^2$ thick, self-supporting 99.9 % enriched ^{24}Mg target mounted at the center of the 2 meter diameter scattering chamber “chambre 2000”. During the course of the experiment the reaction products were detected, in singles mode, with four movable small size $\Delta\text{E-E}$ telescopes (displaced in the -7° to -45° angular range with 1° step increments), each consisting of a gas ionization chamber (IC) filled with CF_4 gas at a pressure of 51 Torr and followed by a $500\ \mu\text{m}$ thick Si(SB) detector. The experimental set-up for the coincidence experiment was very similar to that used for the inclusive experiment and consisted of seven ionization-chamber telescopes in the reaction plane between -37° and $+95^\circ$.

The energy calibrations of the IC’s were obtained using elastically scattered ^{35}Cl projectiles from $100\ \mu\text{g}/\text{cm}^2$ thick Au and C targets and from the Mg target, combined with measurements of α sources and a calibration pulser. On an event-by-event basis, corrections were applied for energy loss in the targets and in the entrance window foils on the IC’s and for the pulse height defect in the Si detectors [30]. The thicknesses of the C contaminants were experimentally estimated to be less than $10\ \mu\text{g}/\text{cm}^2$ by using α backscattering techniques. To correct for the C contamination, measurements were also performed with the C target [24] at the same position settings with similar beam conditions. The absolute normalization of the measured differential cross sections was determined from an optical model analysis of the elastic scattering measured at the more forward angles using potential parameters found to fit accurately the lower energy data for the same reaction [31].

III. EXPERIMENTAL RESULTS

Inclusive kinetic-energy distributions were measured for each fragment produced in the $^{35}\text{Cl}+^{24}\text{Mg}$ reaction at $E_{lab} = 275$ MeV for each detection angle. The heaviest fragments have typical ER energy spectra arising from the statistical decay of the fully equilibrated CN formed in a CF process as shown in our detailed inclusive measurement performed at $E_{lab} = 282$ MeV [16,17]. It is worth noting that, according to the fusion systematics of Morgenstern and collaborators [32], 6.4 % of the observed ER yield is expected to arise from an incomplete fusion (ICF) process. This is verified by the extraction of the mean velocities of the ER's which do not deviate significantly (less than 1 or 2 %) from the expected velocity of the recoiling CN [33].

The kinetic-energy distributions of the lightest of the fragments ($5 \leq Z \leq 12$) which were detected at -7° are shown in Fig.1. They have characteristic Gaussian shapes whose centroids correspond to binary-breakup processes with full energy damping, consistent with the systematics of **light** heavy-ion fission reactions [10]. The dashed lines are the results of a statistical-model calculation which will be described in the following Section.

The centroids of the inclusive energy distributions were extracted for each charge number ($Z \leq 12$) in order to deduce their total kinetic energy (TKE) values assuming two-body kinematics in the center-of-mass (c.m.) frame. The results are shown in Fig.2. The very weak dependences of the TKE values and of the differential cross sections $d\sigma/d\theta$ (see Ref. [33]) on the scattering angle for each exit channel indicate that the lifetime of the di-nuclear complex is longer than the time needed to fully damp the energy in the relative motion of FF and DI processes. The extracted average TKE values are also plotted in the insert of Fig.2 as a function of Z . The dashed and solid lines (in the insert) are the results of a calculation of a FF model which will be developed later. Furthermore the average TKE value corresponding to symmetric-mass splitting is close to the predictions of the recent extension of the Viola systematics to light nuclei [10].

The TKE distributions were also deduced for all the binary fragments from the angular correlation coincidence data as shown in Fig.3. Depending of the chosen angle settings, events arising from quasi-elastic to fully energy-damped processes are selected by the coincidence requirements ; i.e. the more the folding angle (which is defined as being the separation angle between coincident fragment pairs) is open, the more the collision is peripheral [34] with smaller linear-momentum transfer. The circles which illustrate a full energy damping were deduced from the TKE systematics of Ref. [10]. From a comparison of the mean locus of experimental TKE values with the indicated circles it is clearly visible that the fission fragments need optimum values for the folding angles as it is well known for FF reactions of heavy-mass systems [34].

Integrated cross sections of the inclusive measurements are given in TABLE I in comparison with the results obtained at a slightly higher bombarding energy $E_{lab} = 282$ MeV [16,17]. Both sets of data show quite comparable results as expected for very close bombarding energies. The experimental elemental Z distribution (full points) of the integrated fully-damped yields (for $Z \leq 12$) and ER cross sections are plotted in Fig.4 with two statistical-model calculations (full and dashed histograms) which will be discussed in detail in the next Section. Only those nuclei with nuclear charge near that of the projectile have kinetic energy distributions indicative of a mixture of mechanisms. Because of the potential mixing with large DI components [33] (which might be composed of either partially damped or fully-damped yields), no attempt was undertaken in order to extract the FF yields for $Z = 13$ to 15 and the ER yields for $Z = 16$ and 17 at this energy. This difficulty has been successfully addressed by Cavallaro et al. [16,17] at 282 MeV and the final results are also given in TABLE I.

The total FF and ER cross sections are $\sigma_{FF} = 137 \pm 5$ mb (lower limit) and $\sigma_{ER} = 722 \pm 197$ mb respectively in very good agreement with the previously published results [16,17]. The corresponding critical angular momentum is $L_{crit} = 44.6 \pm 5.4 \hbar$ as calculated by using the sharp cutoff approximation. This value is taken as an input parameter of the fusion partial wave distribution needed for the statistical-model calculations which are discussed in the next Section.

The possible occurrence of ternary processes that involve three massive fragments in competition with the binary-decay mechanisms is investigated in the analysis of the fragment-fragment coincidence data. The results of the measured angular correlations are displayed in Fig.5 for the indicated charge partitions and position settings. They are found to peak at relatively well defined angles between $\theta_2 = +40^\circ$ and $+50^\circ$, independently of the charge partition, indicating that the fragments have a dominant two-body nature as expected for bombarding energies lower than 10 MeV/nucleon [24,25,35–37]. The peak positions in the correlation functions may give an estimate of the reaction Q-value for the primary decay. Although we did not perform a quantitative analysis of these correlation functions, the conclusions deduced from the TKE vs Z plots given in Fig.3 are qualitatively well confirmed. Similarly the width of the distributions are correlated to the degree of damping. The effect of secondary light-particle emission will be to broaden these distributions, but without significantly affecting the centroids of the correlations.

In previous experiments using projectiles of mass $A_{proj} = 32$ to 40 on various targets, events corresponding to the emission of three heavy fragments ($A \geq 6$) have been found to occur significantly (at a 10 % level) only at much higher bombarding energies (10-15 MeV/nucleon) [21,38–40]. Sequential fission decay was clearly observed for fragments resulting from reactions of $^{58}\text{Ni}+^{58}\text{Ni}$ at 15.3 MeV/nucleon [20]. More recently, however, there has been evidence cited in the literature [23] for three-body events in ^{32}S induced reactions at lower energies (4-6 MeV/nucleon).

In the following we investigate this possibility of three fragment emission in the present exclusive data through the analysis of the Z_1 - Z_2 coincident yields which were energy integrated for $Z_{1,2} \geq 5$ by using the same procedure that we have developed previously for the $^{35}\text{Cl}+^{12}\text{C}$ reaction [24]. Here Z_1 is the atomic number of the fragment detected in the first telescope and Z_2 is the atomic number of its binary partner which is detected in coincidence in the second telescope on the opposite side of the beam axis. Essentially no coincidences between telescopes on the same side of the beam axis were expected. The Z_1 - Z_2 correlation results are displayed in Fig.6 for the indicated position settings. The diagonal lines given by

$Z_1+Z_2 = Z_{proj}+Z_{target} = Z_{CN} = 29$ correspond to binary reactions with no LCP evaporation. The majority of coincidence events lie in bands corresponding to an approximate constant sum of Z_1 and Z_2 and parallel to the CN diagonal lines. Their maximum yields are found to occur near $Z_{tot} = 25-26$, regardless of whether the exit-mass partition is symmetric or not. However, it is interesting to note that for the -37° correlation plots, the charge deficits are smaller. This is due to the fact that large correlation angles select more peripheral collisions with a smaller energy damping [34] and therefore the sequential LCP and neutron emission is smaller with a moderate linear-momentum transfer. The most probable missing charge $\langle \Delta Z \rangle$ was found to be around 3-4 charge units, which is most likely lost through particle emission from either the excited composite system or a secondary sequential evaporation from one of the binary-reaction partners. Similar conclusions were reached for the $^{35}\text{Cl}+^{12}\text{C}$ reaction [24] at a comparable bombarding energy. To summarize, the correlations between the measured nuclear charges of the two detected fragments allow us to determine that the decay mechanism is predominantly binary. In effect, ternary exit channels would yield events falling far below the observed bands. In order to perform a more quantitative analysis of these processes we plot in Fig.7 and Fig.8 the coincident yields as a function of the missing charge for the chosen position settings. The nuclear charge deficits (missing charges) are used to isolate the exit channels which have a probability of containing three fragments and an unidentified number of light particles. These results are discussed in the next Section.

IV. DISCUSSION

The spectra of the total missing charge, displayed in Fig.7, have typical Poisson-like distributions with a most probable value $\lambda = \langle \Delta Z \rangle$:

$$P(\Delta Z) \propto \lambda^{\Delta Z} e^{-\lambda} / \Delta Z!$$

The corresponding curves by using this expression are also given in the figure. Although the most probable values do not strongly depend on the detector positions (45 different position settings were measured), the angular dependence of these values gives an estimate of the average energy transferred into the fragments according to the two-body kinematics. It should be noted that a non-statistical emission, such as a ternary breakup mechanism, will produce enhanced yields superimposed on the tail of the missing charge distributions at large ΔZ values as shown previously for ^{32}S induced reactions at 10 MeV/nucleon bombarding energies [41]. The data of the individual missing charges of Fig.8 (solid histograms) are furthermore reasonably well reproduced by a statistical-model calculation (dashed histograms) whose results will be discussed later.

An average charge-deficit value of $\langle \Delta Z \rangle = 3.74 \pm 0.22$ is obtained from 30 position settings as selected to take only the fully-damped events into account. This value is appreciably larger than the ones measured for the $^{35}\text{Cl} + ^{12}\text{C}$ at $E_{lab} = 200$ MeV [6] $\langle \Delta Z \rangle = 0.96 \pm 0.12$ and at $E_{lab} = 278$ MeV [24] $\langle \Delta Z \rangle = 1.74 \pm 0.15$. This result confirms that the nuclear charge deficit increases linearly with the c.m. available energy and thus with the total excitation energy in the composite system [37].

To illustrate this results the average charge-deficit values obtained in the present work along with a collection of other data taken from the literature [20,21,35–40] (see TABLE II) were plotted against the c.m. bombarding energy in Fig.9 as first proposed by Winkler et al. [37]. The two $^{35}\text{Cl} + ^{12}\text{C}$ data points [6,24] and the point measured in this work for the $^{35}\text{Cl} + ^{24}\text{Mg}$ reaction are shown as a full cross. The highest energy points ($E_{lab} \approx 15$

MeV/nucleon) which should correspond to a selection of binary breakup events [20,40], with lower charge-deficit values, appear to deviate (within the error bars) from the rest of the data points. At these energies it is believed that approximately 10-30 % of the events contain more than two and more probably three fragments [40]. The other explanation of this deviation from the systematics may arise from the fact that the linear-momentum transfer becomes less complete as expected for pre-equilibrium processes likely to occur at these bombarding energies. With the exception of these high-energy points all the data appear to be well aligned. The linear dependence is fitted for the low-energy data by the following relationship :

$$\langle \Delta Z \rangle = 0.044 (E_{c.m.} - 32.23),$$

where the c.m. energy is in units of MeV. This behaviour is shown as a straight line in Fig.9. An energy threshold of about 32.23 ± 0.5 MeV is found for the emission of light-charged particles and an excitation energy increase of 22.72 ± 1.0 MeV is required on average for the emission of one unit of particle charge in qualitative agreement with previous analyses [37,41]. This should be considered as twice the energy needed to evaporate one unit of mass. Similar conclusions were also reached from inclusive measurements of ER mass distributions [42] and from exclusive measurements on the decay of projectile-like fragments in the intermediate energy domain [43]. These results suggest that a common behaviour of LCP evaporation in low-energy fusion reactions and intermediate-energy projectile breakup and show that in the present case the emission occurs as a statistical evaporation from equilibrated nuclei.

In summary, as for the $^{35}\text{Cl}+^{12}\text{C}$ reaction studied at a comparable bombarding energy, the present $^{35}\text{Cl}+^{24}\text{Mg}$ charge-deficit results are consistent with a statistical decay of binary fragments and follow the proposed systematics for this behaviour quite well, in contrast to the data of [23] whose results are not yet well understood. The absence of ternary events in the present measurement is consistent with results from ^{32}S induced reactions where evidence of three-body processes is only seen at incident energies higher than 10 MeV/nucleon [41]. The proposed systematics calls for subsequent measurements (using the present experimental technique) of the $^{35}\text{Cl}+^{24}\text{Mg}$ reaction at an energy of approximately 12 MeV/nucleon which

could correspond of the threshold of ternary processes. For heavier nuclear systems [19–22] ternary events arise when the reaction proceeds mostly via a sequential two-step mechanism : an initial quasi-elastic or deep-inelastic interaction is followed by the fission-like decay of one of the excited nuclei producing a three-body exit channel in the final state with a reasonable probability. This phenomenon of sequential fission [19] is known to be of importance for very heavy nuclei. On the other hand second chance fission is unlikely to occur for light di-nuclear systems due to the height of the fission barriers [10,29]. Therefore it can be surmised that, in the present experiment, the inclusive cross sections measured for the lightest Z fragments ($Z \leq 12$) arise from a fully-damped binary process, such as FF, followed by a sequential emission of LCP and neutrons. In the subsequent discussion we will consider these binary fragments as the products of a FF process whose properties can be treated by the statistical process.

Two different statistical approaches are used to interpret the present $^{35}\text{Cl}+^{24}\text{Mg}$ experimental data. In lighter systems [1], where the saddle and scission configurations are known to be very close and little damping is expected as the system proceeds between the two, there is little reason to expect a significant difference between calculations done at the saddle point and scission point than for heavier systems where damping can occur. Indeed, calculations based on the saddle point [4] and scission point [29] are found to give equivalent results. Such a comparison has already been established for the $^{35}\text{Cl}+^{12}\text{C}$ reaction [10]. Both calculations start with the CN formation hypothesis and then follow the system by first chance binary fission or LCP emission and subsequent light-particle, neutron and/or photon emission.

The first model are for calculations based upon the transition-state theory [4,44] and for which the fission width is assumed to depend on the available phase space of the saddle point. Calculations have already been performed for a previous publication [16,17]. In the following the full transition-state model calculations with sequential decay and using the GEMINI code [44] will be labeled as TSM. The main limitation of this code is the lack of reasonable mass-asymmetry dependence of the fission barriers for light nuclei.

The second model corresponds essentially to an extension of the Hauser-Feshbach formalism [29] which treats γ -ray emission, light-particle (n, p, and α) evaporation and FF as the possible decay channels in a single and equivalent way. The Extended Hauser-Feshbach Method (EHFM) assumes that the fission probability is proportional to the available phase space at the scission point. In the following we present the full procedure of EHFM, including secondary emission, which will be called EHFM+CASCADE.

The EHFM+CASCADE approach uses the phase space at the scission point to determine relative probabilities. In the EHFM+CASCADE calculations the scission point can be viewed as an ensemble of two, near-touching spheres which are connected with a neck degree of freedom. The value of the neck length parameter (or separation distance) was chosen to be $s = 3.85$ fm for the $^{35}\text{Cl}+^{24}\text{Mg}$ reaction. This value fits well the systematics dependence $s = 3.5 \pm 0.5$ fm which comes from the literature [6,18,24,29] for the mass region of interest. The large value of s used for the neck length mimics the finite-range and diffuse-surface effects [10] of importance for the light-mass systems [24] and, as a consequence, this makes the scission configurations closely resemble the saddle configurations. A systematic study of a large number of systems [29] allows the parameters of the model to be fixed so as to achieve good agreement with the experimental results. Recent studies [18,24,29] in the framework of EHFM+CASCADE have led to scission configurations being deduced for the lighter systems under study.

In EHFM+CASCADE the calculations are performed by assuming first chance fission which is then followed by a sequential emission of LCP and neutrons from the fragments. Second chance fission is found, as expected, to be negligible in this mass region [25] and, therefore, pre-scission emission was not taken into account in the decay process. The results of the calculated post-scission emission are illustrated by the dashed histograms in Fig.8 by a comparison with the experimental data (solid histograms).

The input parameters of EHFM+CASCADE and TSM are basically the same. In each case, the diffuse cut-off approximation was assumed for the fusion partial-wave distribution using a diffuseness parameter of $\Delta = 1\hbar$ and a L_{crit} value as calculated from the experimental

total fusion cross section given in the previous Section.

The predictions of both approaches can be compared to fully-damped and ER yield data in Fig.4. TSM predictions (dashed histograms) for $Z \leq 15$ are not found to be as good as in the case of the EHF+CASCADE calculations (full histograms). The TSM calculates too high FF cross sections due to a possible overestimation of the centrifugal potential [6]. One possible improvement would be the inclusion of the angular momentum dependent asymmetric fission barriers proposed by Sanders for light nuclei [4]. The disagreement between the EHF+CASCADE calculations and the ER experimental results has been discussed by Cavallaro et al. [17]. The charge-deficits predictions of EHF+CASCADE and TSM displayed in Fig.10 provide both a quite satisfactory agreement of the general trends of the $^{35}\text{Cl}+^{24}\text{Mg}$ and the $^{35}\text{Cl}+^{12}\text{C}$ experimental data. This might be a good indication of the validity of the hypothesis that the saddle-point shape almost coincides with the scission point configurations in this mass region as shown previously in the literature [1,4,24,29].

Since the EHF+CASCADE and TSM approaches are both able to provide reasonably good predictions, we now discuss more deeply the calculated results of EHF+CASCADE. EHF+CASCADE is capable of predicting not only the fission fragment and ER yields which are plotted in Fig.4, but also the FF kinetic-energy distributions and their TKE mean values as shown in Figs. 1 and 2 respectively. Experimental mean $\langle Z_1 + Z_2 \rangle$ values as plotted in Fig.10 are also very well described by EHF+CASCADE calculations using two sets of different level density parameters described later in the discussion.

It was shown that the initial results of EHF+CASCADE [29] were not able to reproduce the measured missing charge distributions and their mean values in the region $Z_1 = 13$ to 16 [18] so well; therefore we need to carefully investigate the possible origins of the observed discrepancies. By using the results of the analysis of the $^{35}\text{Cl}+^{12}\text{C}$ reaction [24], it was first verified that the ^{12}C contamination in the ^{24}Mg target cannot explain the main differences. We can then discuss more deeply the ingredients of the statistical model. During the course of the CASCADE-decay of the primary binary fragments as populated with high excitation energies and high spins, a wide range of nuclei are produced after sequential emissions of

light particles with different excited states until complete cooling of the residual fragments at the end of the cascade chain. It is clear that the decaying fragments are produced with large deviations around averaged values and simplified parametrizations in the decay process.

In the first version of EHF_M+CASCAD_E [29], the measured ground state binding energies are used to evaluate the excitation energy of the decaying fragment, but an average level density parameter was introduced. However two sets of parametrizations are available for the level density parameter a used in each step of EHF_M+CASCAD_E. A constant $a = A/8$ value was chosen for the preliminary calculations of the $^{35}\text{Cl}+^{24}\text{Mg}$ reaction published in Ref. [18]. This parameter set may overestimate shell effects. An alternative way to reproduce the strong variation from fragment to fragment would then be to incorporate shell effects in the level density formulas as proposed by Ignatyuk and co-workers [45–47]. Different descriptions of the temperature and mass dependences of the level density parameter have been recently discussed by several authors [48–50]. In the present work shell corrections in the energy-dependent (temperature-dependent) level density parameter a are produced by the difference of the experimental mass and the liquid drop mass for each fragment. In order to introduce the shell effects in the level density parameter a , we use the empirical formula which is a modification of the simplified form [51] proposed in Ref. [52]. The formula evaluates the shell structure energy which depends on the nuclear temperature T and consequently the level density parameter $a(T)$ becomes nuclear temperature dependent. To get the shell structure energy of the ground state, we use [53] the measured ground state binding energies and the liquid drop binding energies. This new modelization is currently being developed and will be discussed with the original EHF_M+CASCAD_E parametrization [29] in more detail in a forthcoming publication [53]. Preliminary results are however given thereafter.

As a matter of fact it is clearly shown thereafter that one of the possibilities to improve the calculations is to introduce the temperature dependence of the level density parameter a as $a = a(T)$ [52,53]. The comparison is illustrated in Fig.10 where the calculations using a constant level density parameter equal to $A/8$ are given by the dashed line and the

temperature dependent calculations are given by the solid line. As already shown previously in Ref. [18] a discrepancy occurs in the region $Z_1 = 13$ to 16 but does not reappear with the temperature-dependent calculations. The agreement is almost perfect in this latter case. This improvement is confirmed for other quantities such as TKE's, cross sections etc ... as shown in Figs. 2,4,5 and 8 for which the EHF+CASCADE calculations were performed by using the temperature-dependent level densities. At present the reasons for the observed improvement is not yet fully well known but work is in progress [53] for a systematic understanding of this behaviour.

V. CONCLUSIONS

To summarize, the reaction products from the $^{35}\text{Cl}+^{24}\text{Mg}$ system were investigated in detail at the bombarding energy $E_{lab} \approx 8$ MeV/nucleon both with inclusive and exclusive measurements in the framework of a systematic study of the fusion-fission process in light composite systems [1,3–7,15–18,24].

The experimental inclusive data are consistent with previously published inclusive results [15–17] of the study of the $^{35}\text{Cl}+^{24}\text{Mg}$ reaction and provide further important informations on the properties of both the evaporation residues and the binary-decay fragments. Their yields are, for instance, successfully described by statistical models based on either the saddle point picture [4] or the scission point picture [29]. This makes the hypothesis of the fully-damped fragments as being due, to a large extent, to a FF process quite reasonable in accordance with previous systematic studies [1,10,12].

The coincidence data do not show any strong evidence for the occurrence of three-body processes in the $^{35}\text{Cl}+^{24}\text{Mg}$ reaction, in contrast to recent observations for a similar system as studied at a comparable low bombarding energy. The nuclear-charge deficits found in the measurement can be fully accounted for by the sequential evaporation of LCP. This is in agreement with a systematic behaviour that can be established from a compilation of experimental missing charges which have been measured for a large number of reactions studied at bombarding energies below 15 MeV/nucleon. The question of whether or not small parts of the binary reactions actually come from ternary processes is still open and difficult to answer. The energy threshold of ternary processes may be estimated to be approximately 12 MeV/nucleon. Subsequent experimental investigations of the $^{35}\text{Cl}+^{24}\text{Mg}$ and $^{35}\text{Cl}+^{12}\text{C}$ reactions using the present coincidence technique are therefore highly desirable around this threshold energy. However the solution can probably only come from a 4π coverage detector array with high granularity and very small energy thresholds. Thus work is presently in progress with more modest experimental facilities to search for experimental evidence of the

possible occurrence of ternary events in the $^{36}\text{Ar}+^{12}\text{C}$ reaction arising from the breakup of the ^{48}Cr nucleus with a significant population of the $^{16}\text{O} - ^{16}\text{O} - ^{16}\text{O}$ final state [28], possibly indicating an ^{16}O cluster configuration as predicted by both the cluster model [26] and the liquid drop model [27].

In general the measured charge-deficit values and other experimental observables (such as kinetic-energy distributions, elemental cross sections, angular dependence and mean values of the total kinetic energies) are fairly well described by the Extended Hauser-Feshbach statistical-model calculation [29] which takes into account the post-scission LCP and neutron evaporation. This good agreement clearly emphasizes the importance of including a temperature dependence of the level density in statistical-model calculations in **light** di-nuclear systems. Future more refined studies will be undertaken in these directions [53].

ACKNOWLEDGMENTS

The authors wish to thank the Post-accelerated Tandem Service at Saclay for their kind hospitality and the technical support.

REFERENCES

- ^a Present Address: Department of Chemistry, University of Rochester, Rochester NY 14627, USA.
- ^b Permanent Address: Département de Physique, Université de Nice Sophia-Antipolis, F-06034 Nice, France.
- ^c On leave from the Faculty of Textile Science and Technology, Shinshu University, Ueda, Nagano, 386, Japan, as an Overseas Research Scholar of Japan.

- [1] Sanders, S.J., Szanto de Toledo, A., Beck, C.: Phys. Rep. (1998), submitted for publication
- [2] Sanders, S.J., Kovar, D.G., Back, B.B., Beck, C., Dichter B.K., Henderson, D., Janssens, R.V.F., Keller, J.G., Kaufman, S., Wang, T.F., Wilkins, B., Videbaek, F.: Phys. Rev. Lett. **59**, 2856 (1987)
- [3] Beck, C., Djerroud, B., Heusch, B., Dayras, R., Freeman, R.M., Haas, F., Hachem, A., Wieleczko, J.P., Youlal, M.: Z. Phys. **A - Atoms and Nuclei** **334**, 521 (1989)
- [4] Sanders, S.J.: Phys. Rev. C **44**, 2676 (1991)
- [5] Ray, A., Shapira, D., Gomez del Campo, J., Kim, H.J., Beck, C., Djerroud, B., Heusch, B., Blumenthal, D., Shivakumar, B.: Phys. Rev. C **44**, 514 (1991)
- [6] Beck, C., Djerroud, B., Haas, F., Freeman, R.M., Hachem, A., Heusch, B., Morsad, A., Abe, Y., Dayras, R., Wieleczko, J.P., Matsuse, T., Lee, S.M.: Z. Phys. **A - Atoms and Nuclei** **343**, 309 (1992)
- [7] Beck, C., Djerroud, B., Haas, F., Freeman, R.M., Hachem, A., Heusch, B., Morsad, A., Vuillet-A-Cilles, M.: Phys. Rev. C **47**, 2093 (1993)

- [8] Hasan, A.T., Sanders, S.J., Farrar, K.A., Prosser, F.W., Back, B.B., Betts, R.R., Freer, M., Henderson, D.J., Janssens, R.V.F., Wuosmaa, A.: Phys. Rev. C **48**, 1031 (1994)
- [9] Anjos, R.M., Added, N., Carlin, N., Fante, Jr., L., Figueira, M.C.S., Matheus, R., Szanto, E.M., Terein, C., Szanto de Toledo, A., Sanders, S.J.: Phys. Rev. C **49**, 2018 (1994)
- [10] Beck, C., Szanto de Toledo, A.: Phys. Rev. C **53**, 1989 (1996)
- [11] Farrar, K.A., Sanders, S.J., Dummer, A.K., Hasan, A.T., Prosser, F.W., Back, B.B., Bearden, I.G., Betts, R.R., Carpenter, M., Crowell, B., Freer, M., Henderson, D.J., Janssens, R.V.F., Khoo, T.L., Lauritzen, T., Liang, Nisius, D., Wuosmaa, A., Beck, C., Freeman, R.M., Cavallaro, Sl., Szanto de Toledo, A.: Phys. Rev. C **54**, 1249 (1996)
- [12] Szanto de Toledo, A., Carlson, B.V., Beck C., Thoenessen, M.: Phys. Rev. C **54**, 3290 (1996)
- [13] Bhattacharya, C., Bandyopadhyay, D., Krihsan, K., Basu, S.K., Bhattacharya, S., Murthy, G.S.N., Chatterjee, A., Kailas, S., Singh, P.: Phys. Rev. C **54**, 3099 (1996)
- [14] Szanto de Toledo, A., Sanders, S.J., Beck, C.: Phys. Rev. C **56**, 558 (1997)
- [15] Beck, C., Mahboub, D., Nouicer, R., Djerroud, B., Freeman, R.M., Haas, F., Hachem, A., Cavallaro, Sl., De Filippo, E., Di Natale, E., Lanzasó, G., Pagano, A., Sperduto, M.L., Dayras, R., Berthoumieux, E., Legrain, R., Pollaco, E.: Proc. of the XXXIII Intern. Winter Meeting, Bormio, 1995, ed. I. Iori, Ricerca Scientifica ed Educazione Permanente Supp. **101**, 127 (1995)
- [16] Cavallaro, Sl., Beck, C., Berthoumieux, E., Dayras, R., De Filippo, E., Di Natale, E., Djerroud, B., Freeman, R.M., Hachem, A., Haas, F., Heusch, B., Lanzasó, G., Legrain, R., Mahboub, D., Morsad, A., Pagano, A., Pollacco, E., Sanders, S.J., Sperduto, M.L.: Nucl. Phys. **A583**, 161 (1995)

- [17] Cavallaro, Sl., De Filippo, E., Lanzaó, G., Pagano, A., Sperduto, M.L., Dayras, R., Legrain, R., Pollacco, E., Beck, C., Djerroud, B., Freeman, R.M., Haas, F., Hachem, A., Heusch, B., Mahboub, D., Morsad, A., Nouicer, R., Sanders, S.J.: Phys. Rev. C **57**,731 (1998)
- [18] Nouicer, R., Beck, C, Mahboub, D., Matsuse, T., Djerroud, B, Freeman, R.M., Hachem, A., Cavallaro, Sl., De Filippo, E., Lanzaó, G., Pagano, A., Sperduto, M.L., Dayras, R., Berthoumieux, E., Legrain, R., Pollacco, E.: Z. Phys. **A - Atoms and Nuclei** **356**, 5 (1996)
- [19] Glässel, P., v. Harrach, D., Specht, H.J., Grodzins, L.: Z. Phys. **A - Atoms and Nuclei** **310**, 189 (1983) and references therein
- [20] Awes, T.C., Ferguson, R.L., Novotny, R., Obenshain, F.E., Plasil, F., Rauch, V., Young, G.R., Sann, H.: Phys. Rev. Lett. **55**, 1062 (1985)
- [21] Pelte, D., Winkler, U., Gnirs, M., Gobbi, A., Hildenbrand, K.D., Novotny, R.: Phys. Rev. C **39**, 553 (1989)
- [22] Charity, R.J. et al.: Z. Phys. **A - Atoms and Nuclei** **341**, 53 (1991)
- [23] Boccaccio, P., Bettiolo, M., Doná, R., Vannucci, L., Ricci, R.A., Vannini, G., Massa, I., Coffin, J.P., Fintz, P., Guillaume, G., Jundt, F., Rami, F., Wagner, P.: Z. Phys. **A - Atoms and Nuclei** **354**, 121 (1996), and references therein
- [24] Beck, C., Mahboub, D., Nouicer, R., Matsuse, T., Djerroud, B., Freeman, R.M., Haas, F., Hachem, A., Morsad, A., Youlal, M., Sanders, S.J., Dayras, R., Wieleczko, J.P., Berthoumieux, E., Legrain, R., Pollacco, E., Cavallaro, Sl., de Filippo, E., Lanzaó, G., Pagano, A., Sperduto, L.M.: Phys. Rev. C **54**, 227 (1996)
- [25] Murphy, A.St., Le Marechal, R.A., Bennet, S.J., Clarke, N.M., Curtis, N., Freer, M., Fulton, B.R., Hall, S.J., Leddy, M.J., Murgatroyd, J.T., Pople, P.S., Tungate, G., Ward, R.P., Rae, W.D.M., Simmons, P.M., Catford, W.N., Gyapong, G.J., Singer,

- S.M., Chappel, S.P.G., Fox, S.P., Jones, C.D., Lee, P., Watson, D.L.: Phys. Rev. C **53**, 1963 (1996)
- [26] Rae, W.D.M., Merchant, A.C.: Phys. Lett. **B279**, 207 (1992)
- [27] Royer, G.: J. Phys. **G** : Nucl. Phys. **21**, 249 (1995)
- [28] Drummer, A.K., Sanders, S.J., Catterson, T.A., De Lurgio, P.M., Farrar, K.A., Prosser, F.W., Janssens, R.V.F., Wuosmaa, A.H., Beck, C., Szanto de Toledo, A., Added, N.: Bull. Am. Phys. Soc. **42**, 1682 (1997)
- [29] Matsuse, T., Beck, C., Nouicer, R., Mahboub, D.: Phys. Rev. C **55**, 1380 (1997)
- [30] Kaufman, S.P., Steinberg, E.P., Wilkins, B.D., Unik, J., Gorski, A.J., Fluss, M.J.: Nucl. Instr. Meth. **115**, 47 (1974)
- [31] Ferrero, J.L., Pacheco, J.C., Baeza, A., Barrigon, J.M., Bilwes, B., Vinh Mau, N.: Nucl. Phys. **A514**, 367 (1990)
- [32] Morgenstern, H., Bohne, W., Galster, W., Grabisch, K., Kyanowski, A.: Phys. Rev. Lett. **53**, 1104 (1984)
- [33] Nouicer, R.: Ph.D. Thesis, Université Louis Pasteur, Strasbourg, November 1997, Report IReS-97-35
- [34] Viola, Jr., V.E., Back, B.B., Wolf, K.L., Awes, T.C., Gelbke, C.K., Breuer, H.: Phys. Rev. C **26**, 178 (1982)
- [35] Novotny, R., Winkler, U., Pelte, D., Sann, H., Lynen, U.: Nucl. Phys. **A341**, 301 (1980)
- [36] Pelte, D., Winkler, U., Novotny, R., Gräf, H.: Nucl. Phys. **A371**, 454 (1981)
- [37] Winkler, U., Giraud, R., Gräf, H., Karbach, A., Novotny, R., Pelte, D., Strauch, G.: Nucl. Phys. **A371**, 477 (1981)
- [38] Winkler, U., Weissman, B., Bühler, M., Gorke, A., Novotny, R., Pelte, R.: Nucl. Phys.

- A425**, 573 (1984)
- [39] Pelte, D., Winkler, U, Pochodzalla, J., Bühler, M., Gorks, A. Weissman, B.: Nucl. Phys. **A438**, 582 (1985)
- [40] Pelte, D., Winkler, U., Bühler, M., Weissman, B., Gobbi, A., Hildenbrand, K.D., Stelzer, H., Novotny, R.: Phys. Rev. C **34**, 1673 (1986)
- [41] Betz, J., Graff, H., Novotny, R., Pelte, D., Winkler, U.: Nucl. Phys. **A408**, 150 (1983)
- [42] Morgenstern, H., Bohne, W., Grabisch, K., Lehr, H., Stöffler, W.: Z. Phys. **A - Atoms and Nuclei** **313**, 39 (1983)
- [43] Beaulieu, L., Samri, M., Djerroud, B., Auger, G., Ball, G.C., Doré, O., Galindo-Uribarri, A., Gendron, P., Hagberg, E., Horn, D., Jalbert, E., Laforest, R., Larochelle, Y., Laville, J.L., Lopez, O., Plagnol, E., Pouliot, J., Regimbart, R., Roy, R., Steckmeyer, J.C., St-Pierre, C., Walker, R.B.: Phys. Rev. C **51**, 3492 (1995)
- [44] Charity, R.J., Bowman, D.R., Liu, Z.H., McDonald, R.J., McMahan, R.A., Wozniak, G.J., Moretto, L.G., Bradley, S., Kehoe, W.L., Mignerey, A.C.
- [45] Ignatyuk, A.V., Smirenkin, G.N., Tishin, A.S.: Sov. J. Nucl. Phys. **21**, 255 (1975)
- [46] Ignatyuk, A.V., Istekov, K.K., Smirenkin, G.N.: Sov. J. Nucl. Phys. **29**, 250 (1979)
- [47] Grudzevitch, O.D., Ignatyuk, A.V., Plyaskin, V.I., Zelenetsky, A.V.: Proceedings of the International Conference on Nuclear Data for Science and Technology, Mito, Japan, 1988 (unpublished), p.767
- [48] Shlomo, S., Natowitz, J.B.: Phys. Rev. C **44**, 2878 (1991)
- [49] Lestone, J.P.: Phys. Rev. C **52**, 1118 (1995)
- [50] Charity, R.J., Korolija, M., Sarantites, D.G., Sobotka, L.G.: Phys. Rev. C **56**, 873 (1997)

- [51] Bohr, A., Mottelson, B.R.: Nuclear Structure (Benjamin, New York, 1975), Vol.II.
- [52] Matsuse, T., Lee, S.M.: Proceedings of the International Conference on Nuclear Data for Science and Technology, Mito, Japan, 1988 (unpublished), p.699
- [53] Beck, C., Matsuse, T., Nouicer, R.: unpublished

FIGURES

Fig.1 : Experimental (solid lines) inclusive kinetic-energy distributions measured for $Z = 5 - 12$ fragments as produced in the $^{35}\text{Cl}+^{24}\text{Mg}$ at $E_{lab} = 275$ MeV at $\theta_{lab} = -7^\circ$. The dashed lines are the results of the EHF+CASCADE calculations discussed in the text. The results of the calculations are arbitrarily normalized to the data for the sake of clarity.

Fig.2 : Angle dependence of the center-of-mass TKE values for the fully-damped fragments from the $^{35}\text{Cl}+^{24}\text{Mg}$ reaction as measured at $E_{lab} = 275$ MeV. The dashed lines are the EHF+CASCADE predictions discussed in the text. Averaged TKE values are plotted as a function of the atomic number in the insert along with the EHF+CASCADE (solid line) calculations.

Fig.3 : Atomic number dependence of TKE values as deduced from the coincidence measurements of the $^{35}\text{Cl}+^{24}\text{Mg}$ reaction at $E_{lab} = 275$ MeV. The circles correspond to full energy damping of the coincident events. The angle settings of the detectors are defined in the following manner : the first fragment with charge Z_1 is detected at fixed laboratory angles $\theta_1 = -17^\circ$ whereas the second one is detected at variable laboratory angles $\theta_2 = 15^\circ-35^\circ$ (A), $35^\circ-55^\circ$ (B) and $55^\circ-75^\circ$ (C).

Fig.4 : $^{35}\text{Cl}+^{24}\text{Mg}$ elemental distribution (points) measured at $E_{lab} = 275$ MeV compared to two statistical-model calculations discussed in the text. The full and dashed histograms correspond to EHF+CASCADE and TSM calculations respectively.

Fig.5 : $^{35}\text{Cl}+^{24}\text{Mg}$ experimental angular correlations between two heavy fragments with charges $Z_1 \geq 16$ and $Z_2 \geq 5$ measured at $E_{lab} = 275$ MeV. The first fragment is detected at a fixed angle laboratory $\theta_1 = -7^\circ$ whereas the second one is detected at a variable laboratory angle $+17^\circ \geq \theta_2 \geq +80^\circ$.

Fig.6 : Cross sections for coincidence events between two heavy fragments with charge Z_1 and Z_2 measured respectively for $^{35}\text{Cl}+^{24}\text{Mg}$ at $E_{lab} = 275$ MeV for the indicated position settings for which $\theta_1 = -7^\circ$ (a), -17° (b) and -37° (c) in the laboratory system. The size of the squares is linearly proportional to the relative intensity of the pair. The solid lines correspond to binary reactions without LCP emission from the fragments.

Fig.7 : Summed nuclear charge deficits as measured for $^{35}\text{Cl}+^{24}\text{Mg}$ at $E_{lab} = 275$ MeV for the indicated position settings for which $\theta_1 = -7^\circ$ (a) and -17° (b) in the laboratory system. The solid lines are Poisson distribution fits as explained in the text.

Fig.8 : Individual nuclear charge deficits (solid histograms) as measured for $^{35}\text{Cl}+^{24}\text{Mg}$ at $E_{lab} = 275$ MeV for each charge with the chosen position setting. The dashed histograms are the results of the EHF+CASCADE calculations discussed in the text.

Fig.9 : Systematics of the measured nuclear charge deficits. The solid line is the result of a least-square fit procedure discussed in the text. The full points correspond to the data presented in this work, whereas the other open symbols and stars are results taken from other works given in TABLE II.

Fig.10 : Mean $Z_1 + Z_2$ values (experimental points) as measured for :
(a) $^{35}\text{Cl}+^{24}\text{Mg}$ at $E_{lab} = 275$ MeV (present work),
(b) $^{35}\text{Cl}+^{12}\text{C}$ at $E_{lab} = 280$ MeV (Ref. [24]).

TSM calculations (I) and EHF+CASCADE calculations with $a = A/8$ (II) and with $a = a(T)$ (III), including a temperature dependence, are plotted as dotted, dashed and solid lines respectively.

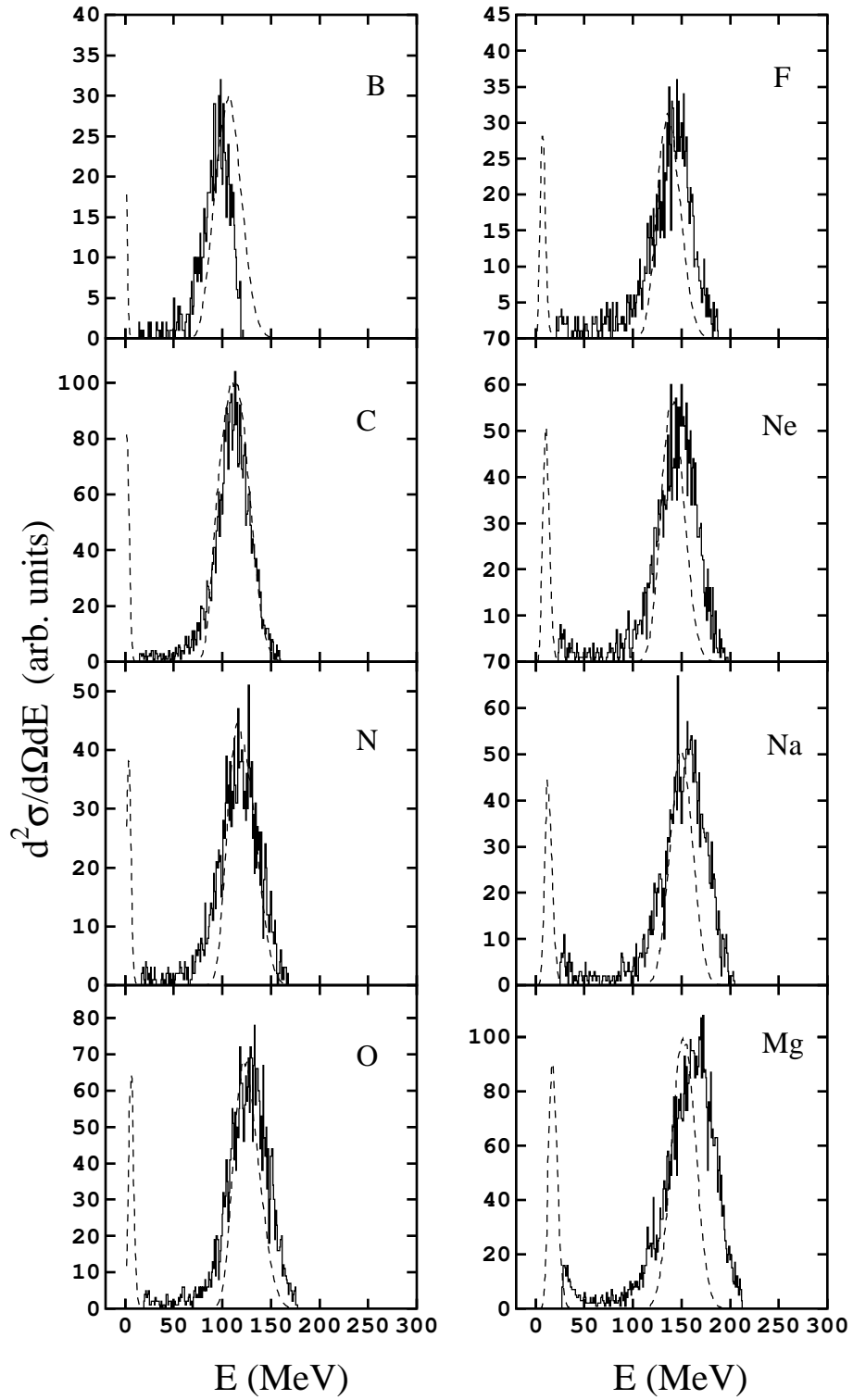
TABLES

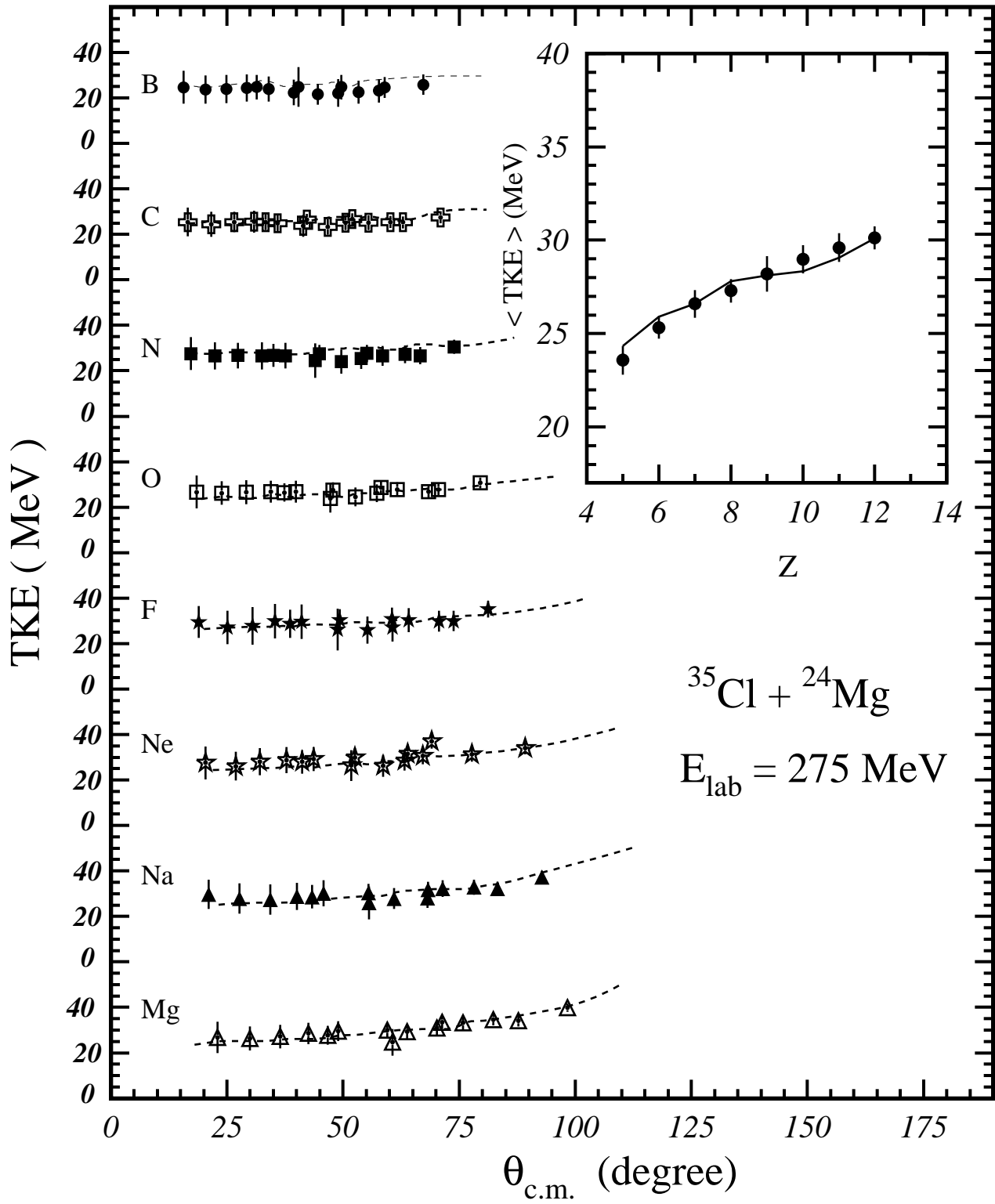
TABLE I. Inclusive fully-damped binary-fragment yields and ER cross sections as measured for the $^{35}\text{Cl}+^{24}\text{Mg}$ reaction respectively at $E_{lab} = 275$ MeV in the present work (a) and at $E_{lab} = 282$ MeV by Cavallaro et al. (b) in the work of Refs. [15] and [16]

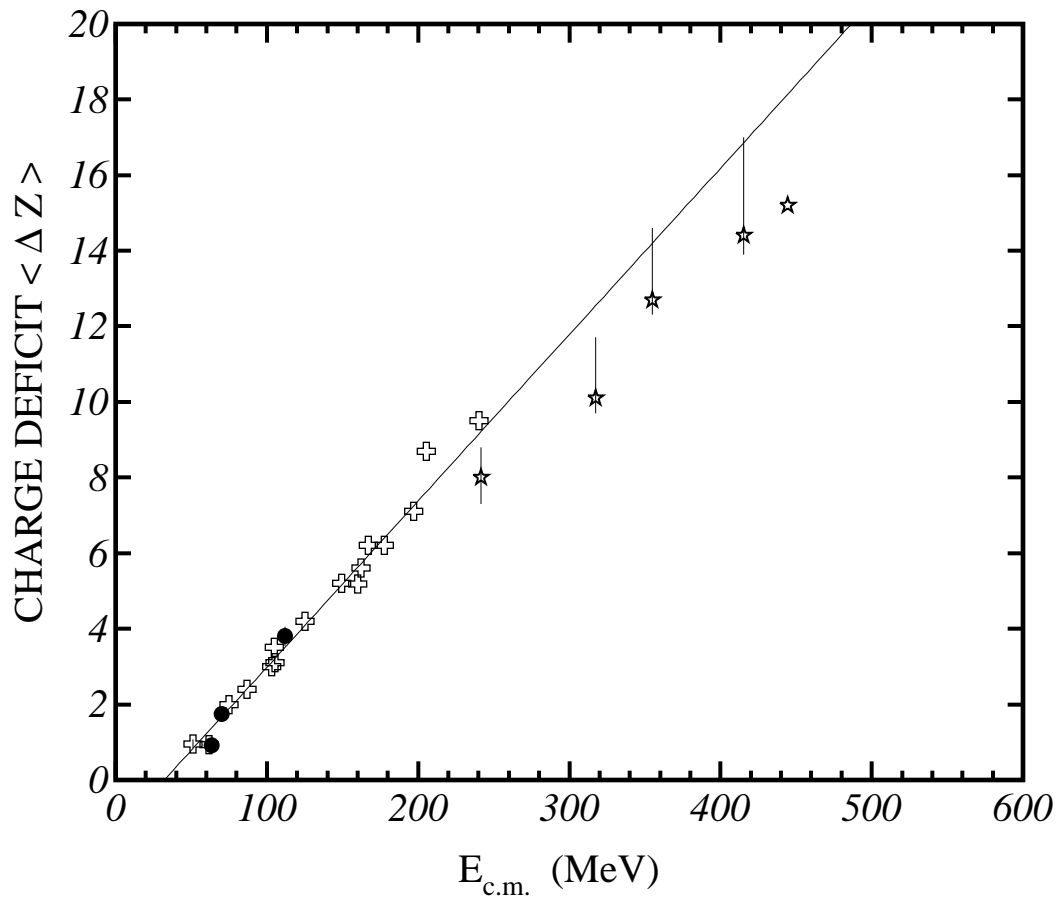
Z	$\sigma_a(mb)$	$\sigma_b(mb)$
3	-	7.2 ± 1.5
4	-	5.9 ± 0.9
5	6.3 ± 0.3	9.7 ± 3.0
6	28.9 ± 1.0	26.9 ± 4.4
7	13.7 ± 0.5	14.3 ± 2.5
8	18.2 ± 1.1	17.2 ± 3.2
9	7.5 ± 0.4	8.5 ± 1.4
10	16.9 ± 0.7	15.2 ± 1.8
11	15.3 ± 0.4	14.1 ± 2.5
12	30.2 ± 0.5	26.6 ± 4.8
13	-	8.8 ± 1.8
14	-	14.0 ± 2.8
15	-	8.0 ± 1.6
16	-	20.0 ± 4.0
17	-	30.0 ± 6.0
18	44.0 ± 9.0	35.0 ± 10.0
19	53.0 ± 10.0	42.0 ± 15.0
20	115 ± 31	110 ± 30
21	149 ± 44	140 ± 50
22	195 ± 53	190 ± 60
23	117 ± 37	90 ± 35
24	49.0 ± 13	42 ± 15

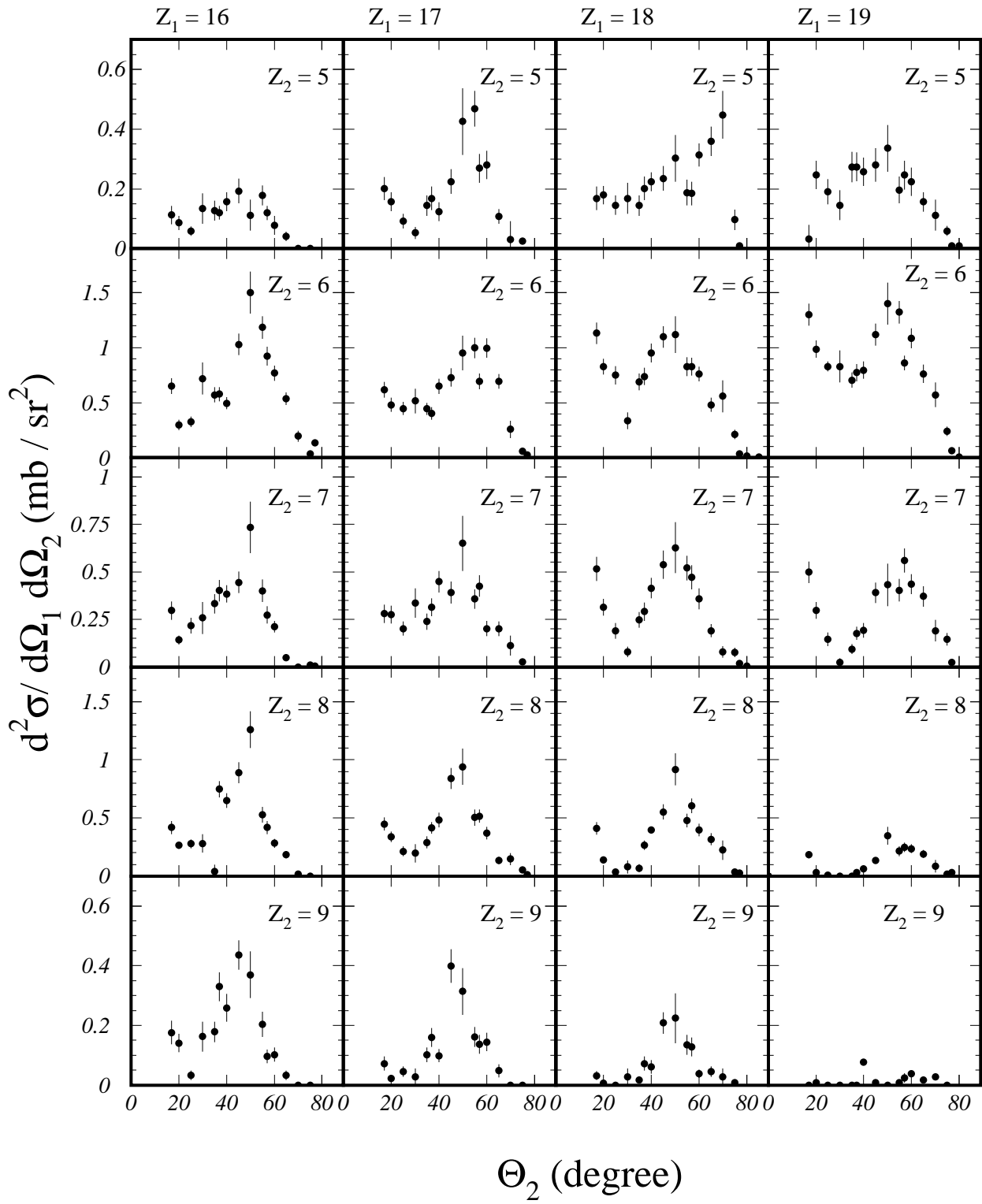
TABLE II. Experimental nuclear charge deficits

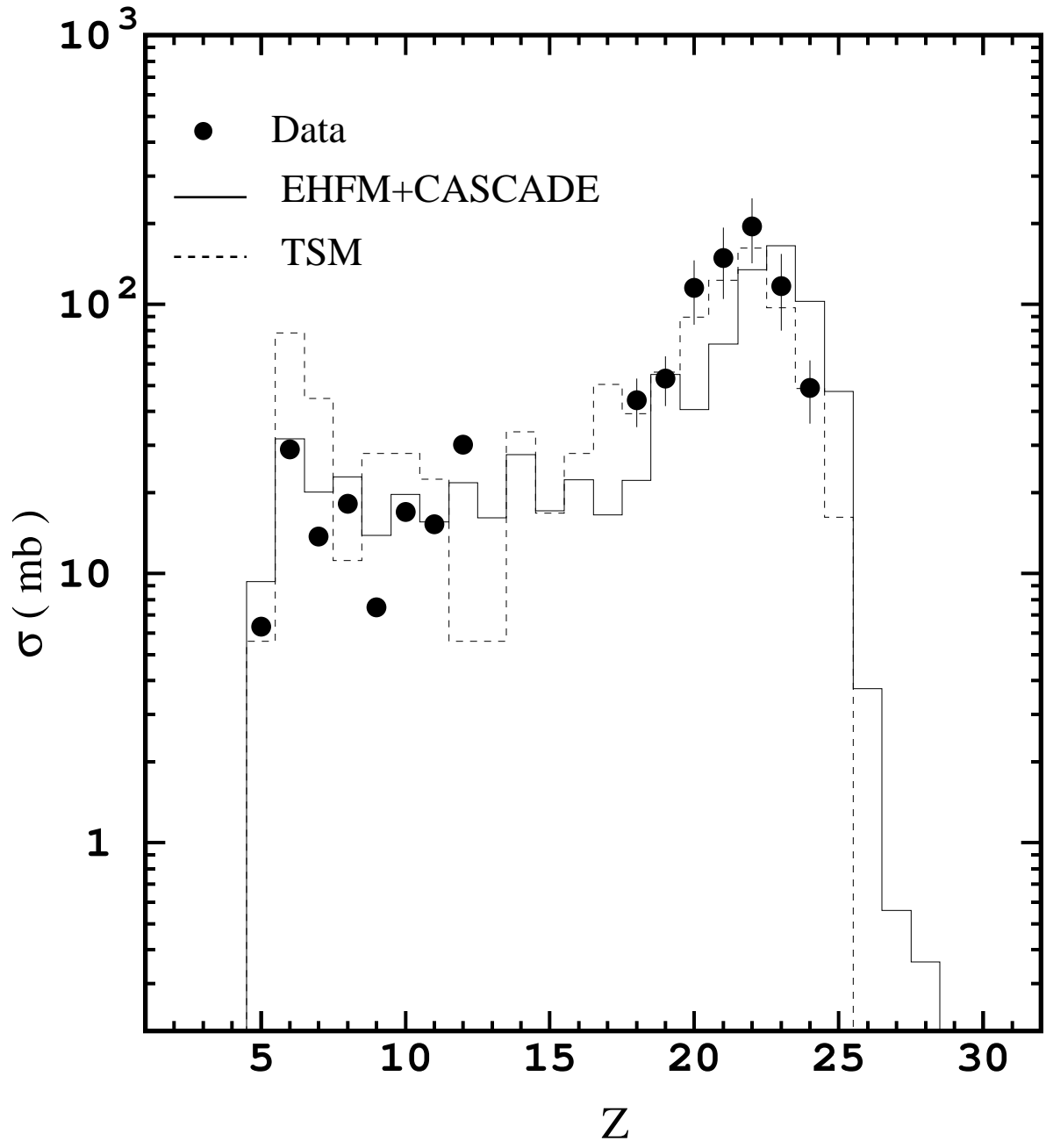
System	E_{lab} (MeV/Nucleon)	$E_{c.m.}$ (MeV)	$\langle \Delta Z \rangle$	Reference
$^{32}\text{S}+^{16}\text{O}$	7.0	75.0	2.0	[37]
$^{32}\text{S}+^{27}\text{Al}$	4.2	61.77	0.93	[36]
$^{32}\text{S}+^{27}\text{Al}$	5.9	86.95	2.40	[36]
$^{32}\text{S}+^{27}\text{Al}$	7.0	102.96	3.0	[37]
$^{32}\text{S}+^{27}\text{Al}$	11.1	162.45	5.6	[38]
$^{32}\text{S}+^{28}\text{Si}$	4.2	63.5	0.91	[35]
$^{32}\text{S}+^{28}\text{Si}$	7.0	105.0	3.5	[37]
$^{32}\text{S}+^{28}\text{Si}$	10.0	149.33	5.2	[41]
$^{32}\text{S}+^{32}\text{S}$	10.0	160.0	5.18	[41]
$^{32}\text{S}+^{40}\text{Ca}$	5.9	105.55	3.1	[37]
$^{32}\text{S}+^{40}\text{Ca}$	7.0	125.0	4.2	[37]
$^{32}\text{S}+^{40}\text{Ca}$	10.0	177.77	6.2	[41]
$^{32}\text{S}+^{40}\text{Ca}$	11.1	197.22	7.1	[38]
$^{35}\text{Cl}+^{12}\text{C}$	5.7	51.06	0.96 ± 0.12	[6]
$^{35}\text{Cl}+^{12}\text{C}$	8.0	70.21	1.74 ± 0.14	[24]
$^{35}\text{Cl}+^{24}\text{Mg}$	8.0	111.86	3.74 ± 0.22	This work
$^{35}\text{Cl}+^{27}\text{Al}$	11.0	167.1	6.2	[39]
$^{35}\text{Cl}+^{40}\text{Ca}$	11.0	205.3	8.7	[39]
$^{35}\text{Cl}+^{58}\text{Ni}$	11.0	240.1	9.5	[39]
$^{40}\text{Ar}+^{27}\text{Al}$	15.0	241.8	$8.0^{+0.8}_{-0.3}$	[40]
$^{40}\text{Ar}+^{45}\text{Sc}$	15.0	317.6	$10.1^{+1.6}_{-0.4}$	[40]
$^{40}\text{Ar}+^{58}\text{Ni}$	15.0	355.1	$12.7^{+1.9}_{-0.4}$	[40]
$^{40}\text{Ar}+^{90}\text{Zr}$	15.0	415.4	$14.4^{+2.6}_{-0.5}$	[40]
$^{58}\text{Ni}+^{58}\text{Ni}$	15.3	444.5	15.5	[20]



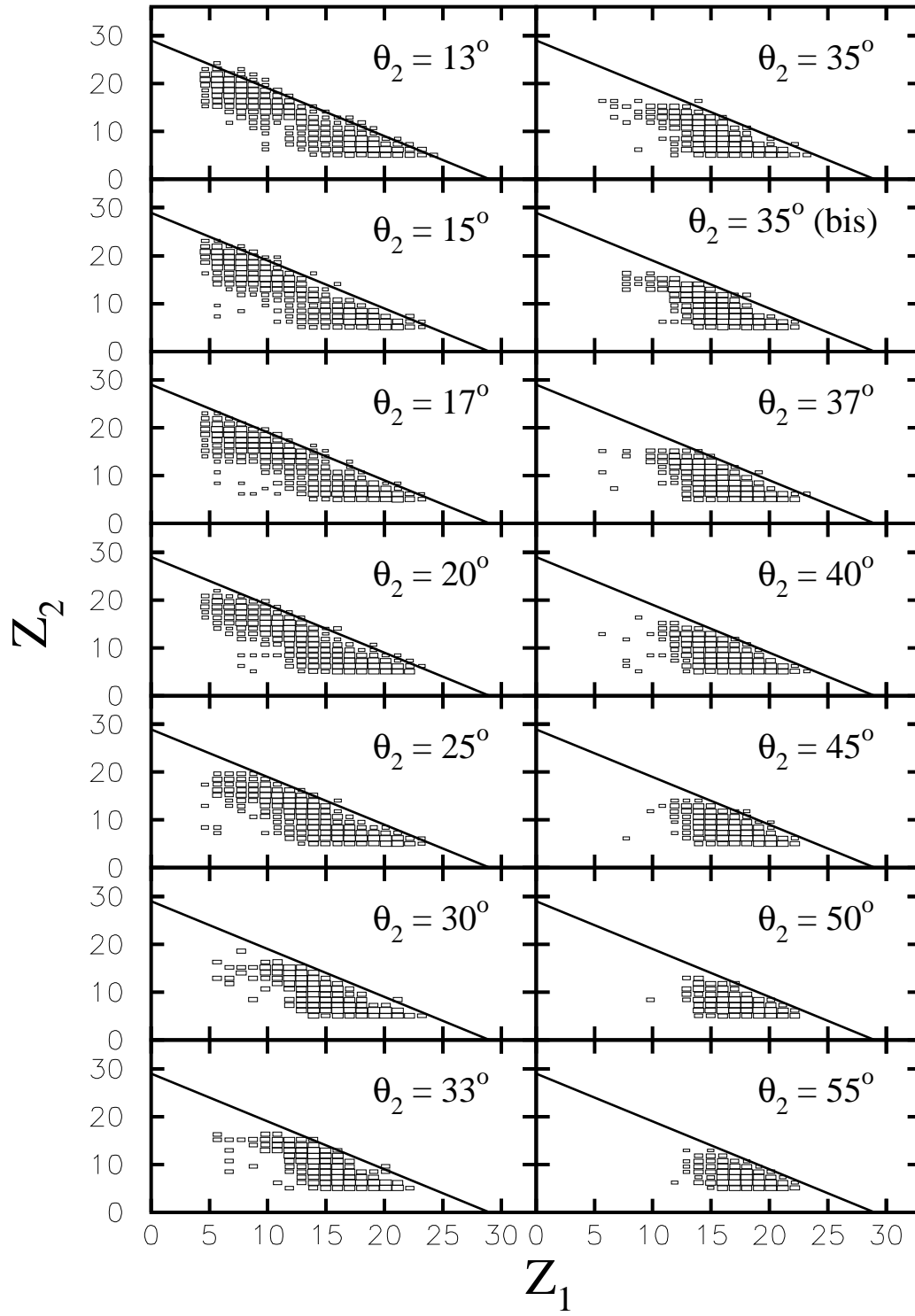








(a)



(b)

